Simple Proofs of a Geometric Property of Four-Bar Linkages

Godfried Toussaint

1. INTRODUCTION. In a planar four-bar linkage (quadrilateral) the angles of the vertices are allowed to change, but the lengths of the edges are preserved during any motion. Consider, for example, the four-bar linkage in Figure 1, where A and B are fixed in the plane. Rotating the bar AD about A causes the bar BC to rotate about B.

[Figure 1 about here]

Such a four-bar linkage has been studied for a long time in the field of kinematics [6], where AD is called the driver, θ is the input angle, and ϕ is the output angle. In this setting only three bars move. Indeed, in the nineteenth century the four-bar linkage was often called the *three-bar* linkage [4], [23]. If the driver link AD is much shorter than the other three links, then it is free to make full 360 degree turns. On the other hand, if the "floating" link CD is much shorter than the others, the motions of the input and output links are severely restricted. Depending on the relative lengths of the four bars, there are twenty-seven different types of planar four-bar linkages that fall into eight basic categories [17].

In kinematics the main interest has been to use four-bar linkages to generate curves by converting the circular motion of the driver link AD to other types of motions [17]. One of the earliest such linkages (the so-called Watt linkage) was patented by the engineer James Watt in 1784 [15]. It was designed to produce nearly straight lines and applied to his steam engines. The Watt linkage is depicted in Figure 2, where AD acts as the fourth link. The point P, midway between B and C, moves vertically in a nearly straight line in the neighbourhood of the position shown.

[Figure 2 about here]

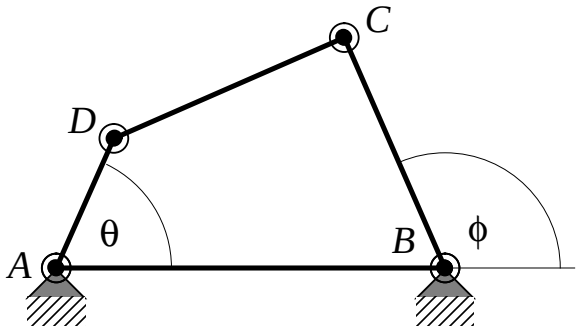

Figure 1: A four-bar mechanism often used in kinematics.

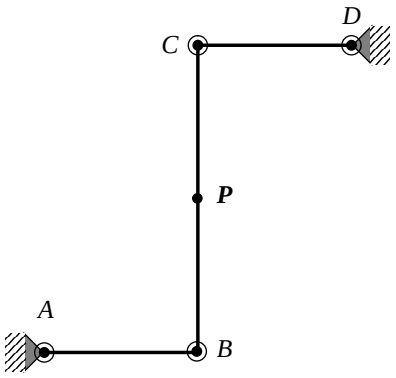

Figure 2: The Watt linkage for nearly straight line motion.

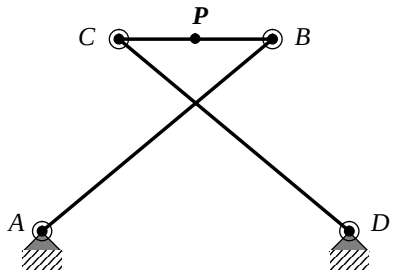

Figure 3: Tchebychef's linkage for nearly straight line motion.

The work of Watt, with its potential for applications in mechanics, generated a flood of activity in the design of mechanisms for generating approximately linear motion. The first mathematician to attack the problem was Tchebychef, a professor at the University of St. Petersburg. His linkage (circa 1850) is depicted in Figure 3, where again AD acts as the fourth link. Here, the point P midway between C and B moves horizontally in a nearly straight line [17].

[Figure 3 about here]

Another mechanism was proposed by Roberts [23] in 1875. Roberts's linkage is radically different from the designs of Watt and Tchebychef, in that the curve is drawn with the aid of the apex of a triangle (the so-called coupler) whose base is attached to the "floating" edge of the linkage. The linkage of Roberts is seen in Figure 4. The point P, the apex of triangle BCP, moves horizontally in a nearly straight line [17]

[Figure 4 about here]

The foregoing linkages can be used to generate a variety of interesting non-linear curves by moving the fixed points A and D closer or further apart, or by changing the lengths of the links. If the Watt linkage is allowed to execute its complete motion, the point P traces out a figure known as Watt's curve. A special case of this curve is the well-known lemniscate of Bernoulli.

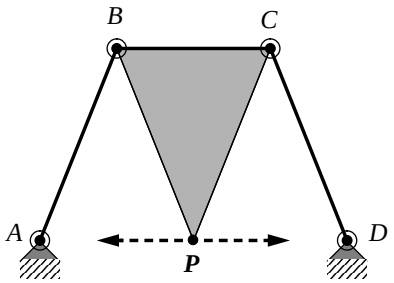

Figure 4: Roberts's linkage for nearly straight line motion.

Furthermore, if the point P is moved away from the center of the link on which it lies, one obtains a more asymmetric variant of Watt's curve, such as the one depicted in Figure 5. Note that the asymmetric figure eight and the circle in which it is enclosed are both part of the curve!

[Figure 5 about here]

A coupler attached to the "floating" edge of the linkage allows the generation of coupler curves of even greater complexity and variety [8]. The Hrones-Nelson book [12] illustrates more than seven thousand different forms of the coupler curve! A particularly simple coupler, depicted in Figure 6, is obtained by extending the segment DC to a point P so that $CP = CB$, and DP is a single rigid bar. If $BC = CD$ and $AB = AD$ the resulting *isoceles* linkage provides an alternate method to generate Bernoulli's lemniscate.

[Figure 6 about here]

The most complicated looking curves are obtained when the coupler is a triangle, as in Roberts's linkage for approximate straight-line motion. With links of suitable lengths and a triangle of suitable size one obtains the curve f with three self-intersections represented in Figure 7. This curve is called the *three-bar sextic curve* by Morley [21] and received much attention in the late nineteenth and early twentieth centuries.

[Figure 7 about here]

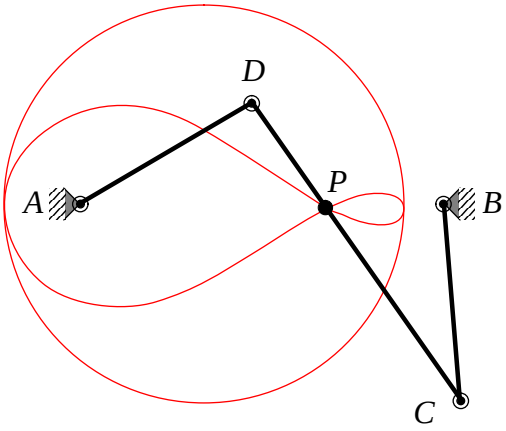

Figure 5: An asymmetric variant of Watt's curve.

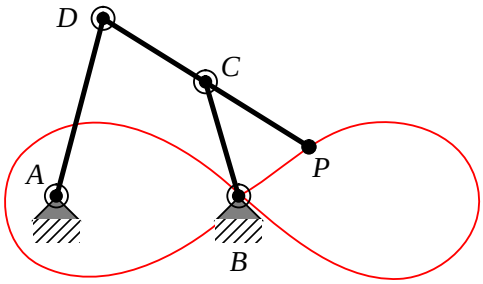

Figure 6: A four-bar linkage with a coupler CP that traces Bernoulli's lemniscate.

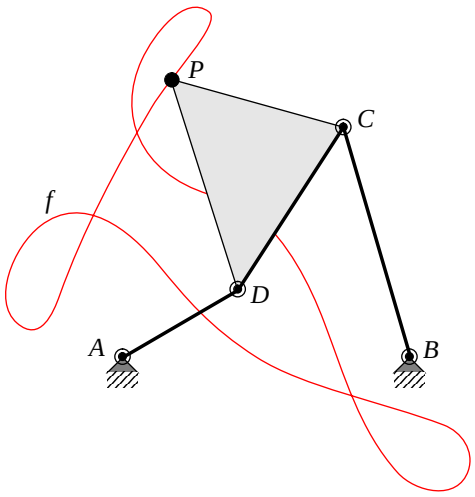

Figure 7: The general sextic coupler curve.

In more recent years there has been growing interest among mathematicians and biologists in describing and visualizing the configuration spaces of these linkages [14], [22], [19]. The configuration space of a linkage is the totality of all its admissible realizations. As an example, consider the four-bar linkage in Figure 1 with link AB fixed and assume that it is a *trapezoidal* linkage with $DA = AB = BC = 1$ and $DC < 1$. Such a linkage is often described in terms of the two angles θ (the *input* angle) and ϕ (the *output* angle) that the rotating links make with the x-axis (the so-called *transmission function*). In [22] and [19] it is proposed to visualize the configuration space of the linkage as a curve in the two-dimensional space of the input and output angles. Such a curve for the trapezoidal linkage is pictured in Figure 8, where the angles θ and ϕ vary from zero to 2π. The curves marked b are for a linkage with the length of $CD \approx 0.85$, whereas those marked a have $CD \approx 0.42$. It is imediately evident from Figure 8 that the curve for such a linkage is made up of two disconnected pieces, implying that the configuration space consists of two disconnected components. Thus there are two configurations of the four-bar linkage with these link lengths such that the linkage cannot move from one configuration to the other while remaining in the plane, without taking the linkage apart.

[Figure 8 about here]

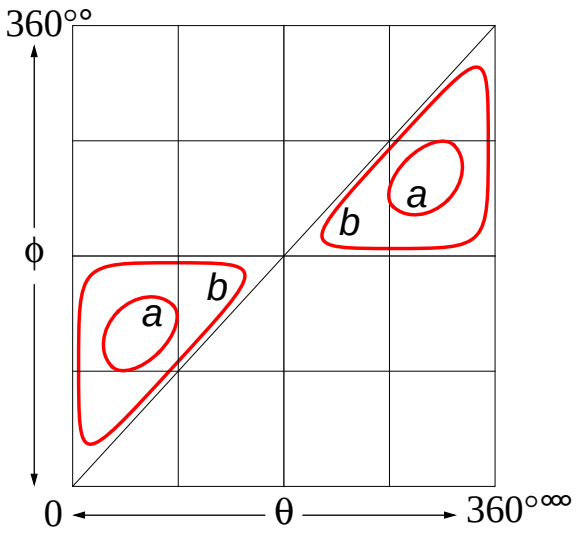

Figure 8: Visualization of the *trapezoidal* four-bar linkage via its transmission function.

As the preceding discussion suggests, the motion of the planar four-bar linkage is well understood and equations describing how any one angle changes as a function of another are readily available [4], [11], [23]. Although the motions of the quadrilateral's edges *relative to each other* do not change when we fix different edges, the behavior with respect to the fixed edge can change radically. For example, as pointed out earlier, in a linkage such as that shown in Figure 1 but with DC much shorter than the other links and AB fixed, the motion of the linkage is severely restricted. Imagine fixing AD instead of AB. Link DC may now realize full rotations about D. This process of changing the fixed edge in a given four-bar linkage is called *inversion* and gives much insight into the overall behavior of the linkage [6]. Additional insight is obtained by analyzing the linkage with a type of inversion that is used frequently in robotics, where it is called a *line-tracking motion* [16]. Consider the four-bar linkage with vertices A, B, C, and D in counterclockwise order as illustrated in Figure 9. Rather than fixing an edge of the linkage, we fix a vertex, say A, and a half-line starting at A and proceeding through the vertex C opposite A. A *line-tracking* motion is realized by translating C along this half-line.

Whereas in the kinematics literature the linkage is analyzed in terms of

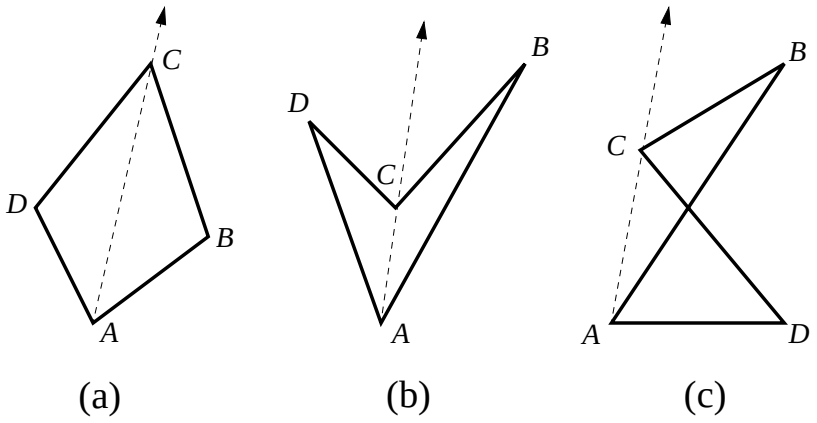

Figure 9: The three types of four-bar linkages: (a) convex, (b) concave, and (c) crossing.

how one angle varies as a function of the angle of an adjacent vertex, one can equivalently analyze the linkage in terms of the lengths of the diagonals. Consider first a two-bar linkage chain ABC. Propositions 24 and 25 of Book 1 of Euclid's *Elements* state that the internal angle at B in triangle ABC increases if and only if the distance between its endpoints A and C also increases [7]. This property of a two-bar chain linkage is also known as the *caliper lemma* [26]. Returning to Figure 9a we see that angle ADC increases if and only if diagonal AC increases, and angle DAB increases if and only if diagonal BD increases. Therefore, instead of examining the behavior of angle DAB relative to angle ADC, we may examine how diagonal DB varies as diagonal AC changes. In the following sections we will make copious use of this caliper lemma without bothering to refer to it every time it is invoked.

[Figure 9 about here]

The fundamental geometric *diagonal-property* of four-bar linkages may be expressed as follows (it is assumed that the linkage is in general position in the sense that no three of its vertices are collinear): *for* convex *and* crossing *four-bar linkages one diagonal increases if and only if the other decreases; for simple* nonconvex *linkages one diagonal increases if and only if the other also increases.*

Although the explicit statement of this property may be novel, the result itself is not new. It is implicit in the complicated equations found in most kinematics books that relate adjacent angles of the linkage [17]. In fact, explicit elementary proofs of the diagonal-property have been published for both convex [1] and simple nonconvex [3] linkages. In this article several novel and simple proofs of the diagonal-property for all three types of linkages are presented.

For applications of the four-bar linkage to many areas of science and engineering the reader is referred to a rich literature. Four-bar linkages form fundamental components of many machines [6], [12], [17] and biological mechanisms [22].

For example, the *convex* four-bar linkage is popular as a rear suspension frame of mountain bicycles. One such design is depicted in Figure 10. The rear portion of the bicycle forms a four-bar linkage $ABCD$, where A is the location at which the rear wheel is attached. If the front of the bicycle is considered fixed, then so is the link BC. Therefore D is free to rotate about C, and A is free to rotate about B. A spring connecting f on the front portion of the bike to e on link CD of the linkage acts to dampen the motion of A, thus providing shock absorption.

[Figure 10 about here]

The *crossing* four-bar linkage is present in the human knee joint, where the anterior and posterior *cruciate* ligaments connecting the upper femur and the lower tibia cross each other, as depicted in a lateral view in Figure 11. Here the femur and tibia play the role of the links CB and AD, respectively, in the Tchebychef linkage. This configuration allows the femur to roll on the tibia, thus reducing friction. Some artificial knee joint prosthetics also use the crossing four-bar linkage in their designs [10].

[Figure 11 about here]

The *concave* four-bar linkage is also found in a large variety of biological mechanisms, especially the feeding apparatus of many fishes [22]. For example, the *horse-mackerel* incorporates an *isoceles*, force-amplification linkage depicted in a ventral view in Figure 12. In this linkage $AB = AD$ and $BC = CD$. If we consider A to be fixed on the x-axis, then muscles move C either left or right also along the x-axis, in a line-tracking motion. A horizontal force applied at C results in an amplified vertical force at B and D.

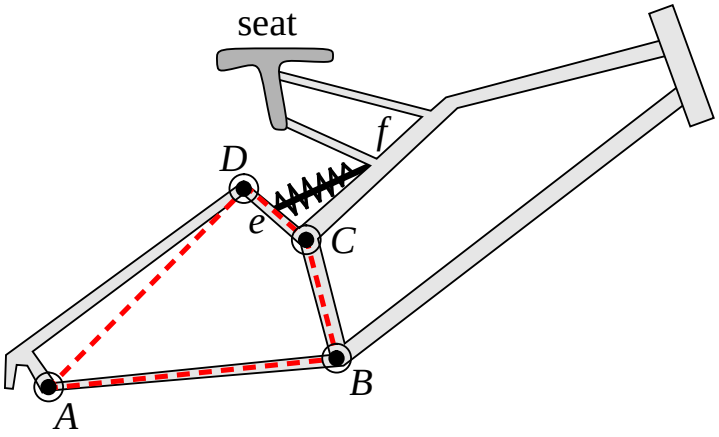

Figure 10: A convex four-bar linkage rear suspension for mountain bikes.

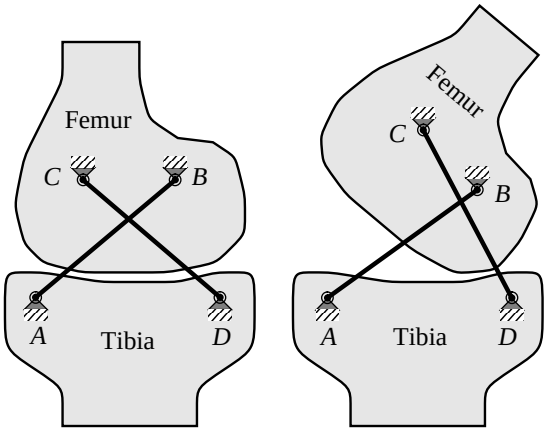

Figure 11: The crossing four-bar linkage in the human knee joint.

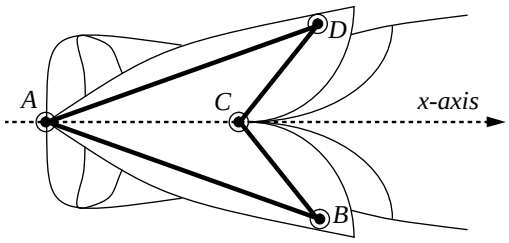

Figure 12: The concave isoceles four-bar linkage in the feeding mechanism of the horse-mackerel fish.

[Figure 12 about here]

The four-bar linkage also offers a relatively simple motion that forms a primitive operation useful for proving more general motions for the reconfiguration of complex multilink linkages. Such linkages serve as models for robot arms [16], [5], knots [20], and molecules arising in both polymer physics [30], [27] and molecular biology [9]. In addition, such primitive motions are used in proving geometric properties about polygons in general [24], [29]. For example, a common problem that arises in these applications is: given two configurations of the same n-bar linkage in $d \geq 2$ dimensions, is it possible to reconfigure one into the other? Several variants of the problem are obtained by specifying which motions are allowed and which constraints must be satisfied. In [24], [20], and [16] the links of the linkage are allowed to self intersect during reconfiguration, whereas in [3] and [5] they are not. The standard technique for establishing that one configuration may be transformed into another is to show that any configuration may be transformed into a *canonical* configuration. One can then follow the path from the first configuration to the canonical configuration, and from there backwards to the second configuration. An attractive canonical configuration for a linkage is one in *convex* position. Thus the crucial problem becomes: given a polygonal linkage $P = (p_1, p_2, ..., p_n)$ in d dimensions, specify a sequence of motions that transforms P into a convex polygon in some plane. Here, the p_i represent the vertices of the polygon, in the same way that the letters A, B, C, and D did in the preceding for the special case of the four-bar linkage. One of the steps repeatedly used in [24] to convexify the linkage P identi-

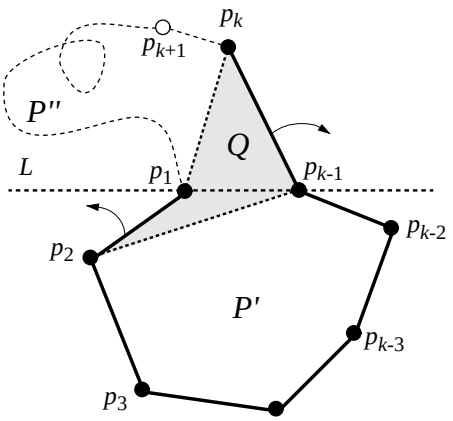

Figure 13: Convexifying a barbed polygon with repeated application of the four-bar mechanism.

fies a portion of P that forms a four-bar linkage, and then convexifies this four-bar portion. To initialize the overall procedure, consider the first three links of the linkage: p_1, p_2, p_3, p_4. Pretend for the moment that (p_1, p_4) is also a link. Therefore $Q = (p_1, p_2, p_3, p_4)$ is a spatial quadrilateral. If Q is not planar, then make it so with a pivot along one of its two diagonals. If Q is not convex, consider it as a four-bar linkage with the diagonal (p_1, p_4) as the fixed edge (the rest of the polygon is connected to the vertices of this edge, p_1 and p_4). This four-bar linkage may now be convexified by rotating one of the bars incident to the fixed phantom edge (p_1, p_4). This procedure yields a plane convex quadrilateral with possibly many more (as yet unexamined) edges connecting p_4 to p_1. The remaining edges are processed one at a time as follows. Advance one edge to p_5 to introduce triangle $T = (p_1, p_4, p_5)$. If T is not coplanar with the quadrilateral Q, then pivot Q about diagonal (p_1, p_4) to make it so. The resulting plane pentagon must now be convexified if it is not convex. Thus every time an edge is advanced, a triangle is "glued" to a growing polygon that is maintained to be convex in some plane.

[Figure 13 about here]

Figure 13 shows one case of this generic step when the vertex p_k is introduced. The portion of the linkage processed thus far, $P_{k-1} = (p_1, p_2, ..., p_{k-1})$,

forms a plane convex polygon. The new vertex p_k introduces a triangle (p_1, p_{k-1}, p_k) separated from P_{k-1} by the line L. A convex polygon with a triangle attached to one of its edges in this way is called a *barbed* polygon. In the case depicted in Figure 13, the polygon $P_k = (p_1, p_2, ..., p_k)$ has two concave vertices at p_1 and p_{k-1}. Therefore one of these, say p_1, may be selected for convexification. To this end, insert a phantom edge (p_2, p_{k-1}) and consider the polygon $P' = (p_2, p_3, ..., p_{k-1})$ as a rigid body attached to (p_2, p_{k-1}). The portion of P not yet processed, $P'' = (p_k, p_{k+1}, ..., p_1)$, is considered to be rigidly attached to (p_k, p_1). The shaded quadrilateral $Q = (p_1, p_2, p_{k-1}, p_k)$ behaves as a planar four-bar linkage. Hence, by rotating (p_2, p_1) counterclockwise about p_2, the angle at p_1 may be straightened. A similar procedure may be used to straighten vertex p_{k-1}, and repeated, if necessary, to convexify the entire polygon P_k, before advancing to the next vertex p_{k+1}.

2. THE CONVEX FOUR-BAR LINKAGE. Aichholzer et al. give in [1] an elementary proof of the diagonal-property for the case of convex linkages. Their proof, however, makes use of the Cauchy-Steinitz lemma [25]. There are many published elementary proofs of this lemma, but most are very long [28]. Even the shortest proof [25], selected for its elegance to adorn the pages of *Proofs from the BOOK* [2] (pp. 64-65), adds unnecessary length, indirectness, and complexity to the proof of the diagonal-property. Here we give two simpler, shorter proofs that do not appeal to the Cauchy-Steinitz lemma.

In the first proof neither an edge nor a vertex is fixed. The proof works just as well for a "floating" linkage.

Consider a linkage $ABCD$ as in Figure 9a. Assume that CA increases. Then the internal angles at B and D must increase. Now the internal angles at A and C cannot remain fixed, for then diagonal DB would remain fixed and the linkage would be rigid, contradicting the fact that AC increases. Therefore the internal angles at A and C either increase or decrease. It is not possible for both angles to increase, because then all four internal angles would increase, violating the fact that the sum of the internal angles of any convex quadrilateral equals 2π. Finally, one angle cannot increase while the other decreases, for by Euclid's caliper lemma, DB would then both increase and decrease simultaneously, which is impossible. Therefore both angles must decrease, causing DB to decrease.

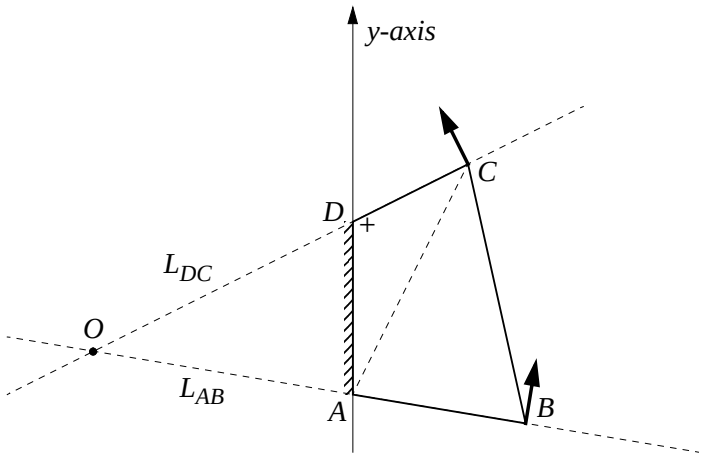

Figure 14: Illustrating the second proof for convex linkages with edge AD fixed via instantaneous centers of rotation.

[Figure 14 about here]

An alternate proof may be obtained by holding edge AD fixed in the plane and using the Descartes principle of instantaneous centers of rotation [18]. Many famous mathematicians, including Descartes, have worked on a class of curves called *cycloids*. When a cyclist rides a bicycle at night with a small phosphorescent spot attached to the rim of one of the wheels, the path that the spot describes as the bicycle moves is a cycloid. According to Melzak [18], Descartes's work on cycloids led him to formulate the following principle: *the instantaneous motion of a plane rigid body moving in its own plane is a rotation about some point (possibly at infinity) acting as the center of rotation.* It should be noted that while Descartes appears to be one of the first to use centers of instantaneous rotations in kinematics problems, the discovery of such a center for *any* motion in the plane is credited to Johann Bernoulli in his 1742 treatise *Opera* [13].

Referring to Figure 14, consider vertex A to be fixed at the origin and assume without loss of generality that vertex D is located on the positive y-axis. In this setting, links AB and DC rotate about A and D, respectively. Consider the direction of instantaneous rotation of the "floating" edge BC. Since AC increases so does angle ADC. In the figures increasing and decreasing angles and diagonals are indicated by "+" and "−" signs, respectively.

Therefore C rotates counterclockwise with respect to D. The locus of centers of instantaneous rotation for C is the line L_{DC} that contains D and C. Similarly, since B rotates about A and moves orthogonally to AB, the locus of centers of instantaneous rotation for B is the line L_{AB} that contains A and B. The intersection point O of these two lines is the instantaneous center of rotation for the edge BC. If O lies to the left of the y-axis as in Figure 14, then the edge BC rotates in a counterclockwise manner with respect to O, as does B with respect to A. If O lies to the right of the y-axis, then the edge BC rotates in a clockwise manner with respect to O, but B still rotates in a counterclockwise manner with respect to A. If O lies at infinity, as happens when DC and AB are parallel, then CD translates in a direction orthogonal to L_{AB} with a positive y-component. In all cases angle BAD decreases. Therefore diagonal DB decreases.

3. THE CROSSING FOUR-BAR LINKAGE. For the crossing four-bar linkage a short and simple proof of the diagonal-property is obtained by fixing one of the edges, say AB as in Figure 15. If diagonal BD increases, then so does angle BAD. Since AB is fixed, it follows that D rotates counterclockwise with respect to A. Now the locus of centers of instantaneous rotations for D is the line containing AD, and for C the line containing CB. Therefore the instantaneous center of rotation for the "floating" edge DC is O, the intersection of the line segments AD and BC. Consequently edge CD rotates counterclockwise with respect to O, whence C rotates counterclockwise with respect to B. Since AB is fixed, angle ABC decreases and diagonal AC decreases with it.

[Figure 15 about here]

4. THE SIMPLE NONCONVEX FOUR-BAR LINKAGE. An elementary but somewhat technical two-page proof of the diagonal-property for simple nonconvex four-bar linkages was given by Biedl et al. [3]. In this section three new proofs are presented. The first, like the proof in [3], holds one edge fixed, but is much simpler.

[Figure 16 about here]

As before, fix edge AD in the plane and refer to Figure 16. If AC increases, then angle ADC also increases, causing C to rotate counterclockwise

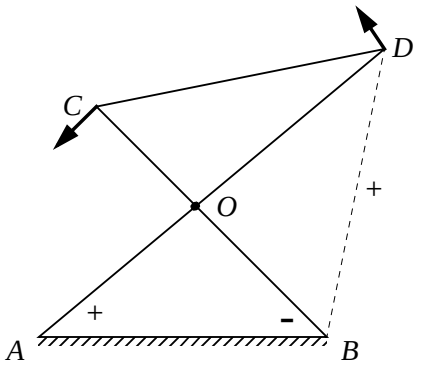

Figure 15: A crossing linkage with edge AB fixed and O as the instantaneous center of rotation of edge CD.

about D. Since C is a concave vertex, the line L_{DC} containing D and C (the locus of centers of instantaneous rotations for C) intersects the segment AB at O, the center of rotation for the "floating" edge BC. Therefore edge CB rotates clockwise with respect to O, forcing B to rotate clockwise with respect to A. But since AD is fixed, angle DAB increases. By the caliper lemma, diagonal DB increases as well, completing the proof.

The second proof, which holds for the line-tracking motions defined in the introduction, is a longer case-analysis, but gives additional insight into the behavior of the linkage by fleshing out the more difficult case in which all four edges rotate in the *same* direction with respect to the plane.

Once again, let C be the concave vertex, let A be located at the origin of the plane, and without loss of generality, let C lie on the positive y-axis (see Figure 17). Since the linkage is not convex, at least one of B or D must lie strictly above the line L_C that runs parallel to the x-axis and contains C. Without loss of generality assume that B lies strictly above L_C.

[Figure 17 about here]

A line-tracking motion moves C along the ray from A in the direction of C, i.e., along the y-axis. Note that the line L_C is the locus of instantaneous centers of rotation for C. Five interesting cases arise depending on whether (1) D lies strictly above L_C, (2) D lies on L_C, (3) D lies below L_C and above the x-axis, (4) D lies on the x-axis, or (5) D lies strictly below the x-axis.

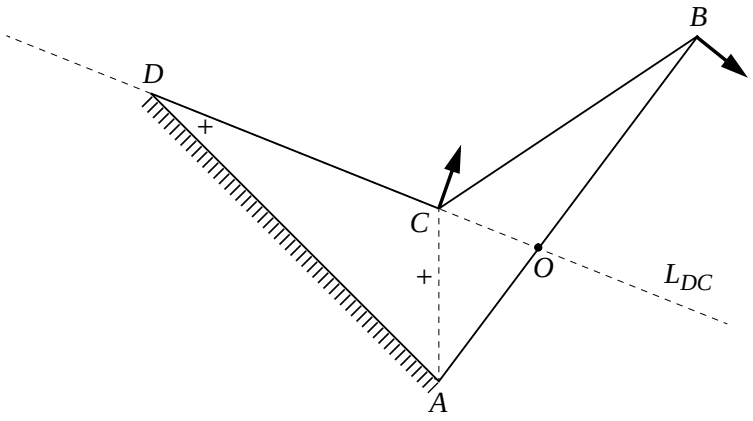

Figure 16: A simple non-convex linkage with edge AD fixed and O as the instantaneous center of rotation of edge BC.

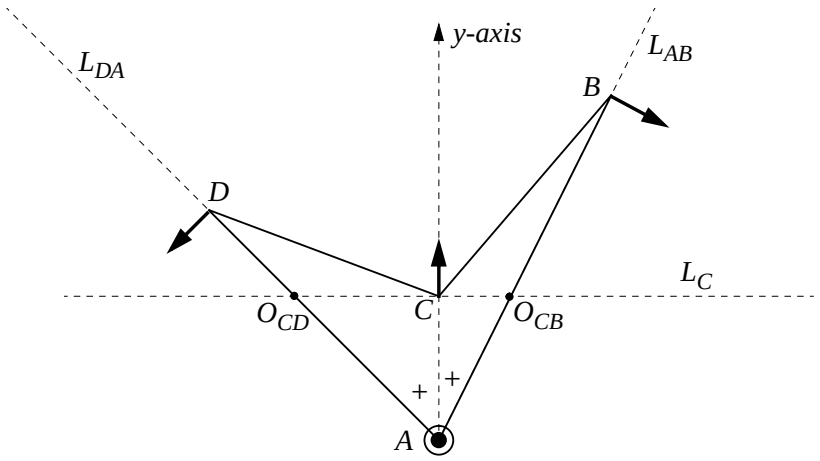

Figure 17: Illustrating the proof for the *line-tracking* motion for Case 1.

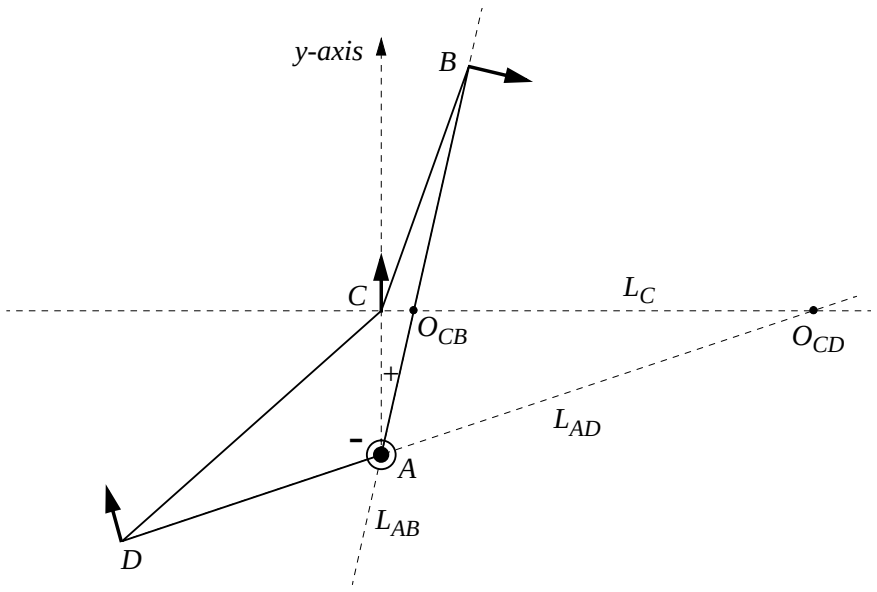

Figure 18: Illustrating the proof for the *line-tracking* motion for Case 5.

Cases 1 and 5 are discussed in what follows. The reader is invited to supply similar proofs for the other three cases.

Consider then Case 1, where D lies strictly above L_C, and refer to Figure 17. In this setting the bars AD and AB rotate about A and the loci of instantaneous rotations for D and B are the lines L_{DA} and L_{AB}, respectively. Since C translates upwards, the edge CD rotates counterclockwise with respect to O_{CD}, its instantaneous center of rotation. Therefore D rotates counterclockwise with respect to A, and angle CAD increases. Similarly, edge CB rotates clockwise with respect to O_{CB}, its instantaneous center of rotation. As a result, B rotates clockwise with respect to A, and angle CAB also increases. This demands that both angle BAD and diagonal BD increase. Note that in this case two edges rotate clockwise, the other two counterclockwise.

For Case 5, where D lies strictly below the x-axis, refer to Figure 18. Now O_{CD}, the instantaneous center of rotation for edge CD, lies to the right of C, making D rotate clockwise with respect to A and thereby forcing angle DAC to decrease. On the other hand, ABC still behaves as in Case 1. Hence the two internal angles at A change in opposite directions. Furthermore, the

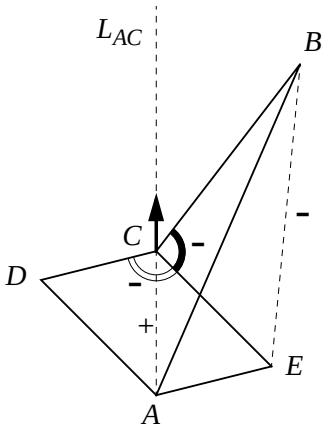

Figure 19: Illustrating the third proof using the six-bar linkage construction.

edges CD and CB are both rotating in the same clockwise direction. This case is more difficult than the others because *all* four edges are rotating clockwise, obscuring what happens to the external angle at C. The reader is invited to verify that edge BC rotates *faster* than edge CD, thus establishing that the external angle at C and the diagonal BD increase.

[Figure 18 about here]

Case 5 suggests a third, more elegant, proof that does not break down into cases and does not require fixing either an edge or a vertex, as in the two previous proofs.

Consider a concave linkage $ABCD$, as before with C the concave vertex. Add a new diad AEC to obtain a six-bar linkage like the one illustrated in Figure 19.

[Figure 19 about here]

This new diad lies on the same side of line L_{AC} as B does, and the lengths of its edges are chosen so that together with D it forms a parallelogram $AECD$. The new diad also forms with B a four-bar crossing sublinkage $ABCE$. The six-bar linkage contains all three types of four-bar sublinkages (convex, concave noncrossing, and crossing). Consider now what happens to

the three four-bar sublinkages in the six-bar linkage when AC increases. In the case of the crossing linkage $ABCE$, it was shown that EB decreases, as does the acute angle BCE. For the convex linkage $AECD$, it was shown that DE decreases, and the acute angle DCE decreases along with it. But these two angles together with the external angle BCD sum to 2π. Therefore the external angle BCD and diagonal BD both increase.

5. ACKNOWLEDGEMENTS. I would like to thank Michael Soss for reading an earler version of this manuscript, Stefan Langerman for providing the figure of the variant of Watt's curve, and the referees for helpful suggestions on improving the exposition of the paper.

References

[1] O. Aichholzer, E. Demaine, J. Erickson, F. Hurtado, M. Overmars, M. Soss, and G. T. Toussaint. Reconfiguring convex polygons. In *Proc. 12th Canadian Conference on Computational Geometry*, pages 17–20, Published by University of New Brunswick, Fredericton, New Brunswick, 2000.

[2] M. Aigner and G. M. Ziegler. *Proofs from THE BOOK*. Springer-Verlag, New York, 1998.

[3] T. Biedl, E. Demaine, M. Demaine, S. Lazard, A. Lubiw, J. O'Rourke, M. Overmars, S. Robbins, I. Streinu, G. T. Toussaint, and S. Whitesides. Locked and unlocked polygonal chains in 3d. In *Proc. 10th ACM-SIAM Symposium on Discrete Algorithms*, pages 866–867, New York, 1999. Association for Computing Machinery. ;long version archived by arXiv.org as arXiv:cs.CG/9910009, 8 October 1999.

[4] A. Cayley. On three-bar motion. *Proc. London Math. Soc.*, 7:136–166, 1876.

[5] R. Connelly, E. Demaine, and G. Rote. Straightening polygonal arcs and convexifying polygonal cycles. In *Proc. Symp. Foundations of Computer Science*, pages 432–442, Redondo Beach, CA, 2000. Computer Society Press.

[6] R. J. Durley. *Kinematics of Machines.* John Wiley and Sons, New York, 1903.

[7] Euclid. *Elements.* Dover, New York, 1956. translated by Sir Thomas L. Heath.

[8] R. T. Farouki. Curves from motion, motion from curves. In *Proc. Conference on Curve and Surface Design*, pages 63–90, Saint-Malo, 1999. Vanderbilt University Press, Nashville, TN.

[9] M. D. Frank-Kamenetskii. *Unravelling DNA.* Addison-Wesley, Reading, MA, 1997.

[10] S. A. Gard, D. S. Childress, and J. E. Uellendahl. The influence of four-bar linkage knees on prosthetic swing-phase floor clearance. *J. of Prosthetics and Orthotics*, 8(2):34–40, 1996.

[11] C. C. Gibson and P. E. Newstead. On the geometry of the planar four-bar mechanism. *Acta Appl. Math.*, 7:113–135, 1986.

[12] J. A. Hrones and G. L. Nelson. *Analysis of the Four-bar Linkage: Its Application to the Synthesis of Mechanisms.* Technology Press of MIT, Cambridge, 1951.

[13] W. W. Johnson. The kinematical method of tangents. *Annals of Math.*, 1(6):131–134, 1885.

[14] M. Kapovich and J. Millson. On the moduli space of polygons in the Euclidean plane. *J. Difffl. Geom.*, 42:133–164, 1995.

[15] D. H. Leavens. Linkages. *Amer. Math. Monthly*, 22:330–334, 1915.

[16] W. J. Lenhart and S. H. Whitesides. Reconfiguring closed polygonal chains in Euclidean d-space. *Discrete and Comp. Geom.*, 13:123–140, 1995.

[17] J. M. McCarthy. *Geometric Design of Linkages.* Springer-Verlag, New York, 2000.

[18] Z. A. Melzak. *Invitation to Geometry.* John Wiley and Sons, New York, 1983.

[19] O. Mermoud and M. Steiner. Visualization of configuration spaces of polygonal linkages. *J. Geom. and Graphics*, 4:147–157, 2000.

[20] K. Millet. Knotting of regular polygons in 3-space. *J. Knot Theory and its Ramifications*, 3:263–278, 1994.

[21] F. V. Morley. The three-bar curve. *Amer. Math. Monthly*, 31:71–77, 1924.

[22] M. Muller. A novel classification of planar four-bar linkages and its application to mechanical analysis of animal systems. *Philosophical Transactions: Biological Sciences*, 351:689–720, 1996.

[23] S. Roberts. Three-bar motion in plane space. *Proc. London Math. Soc.*, 7:14–23, 1875.

[24] G. T. Sallee. Stretching chords of space curves. *Geom. Dedicata*, 2:311–315, 1973.

[25] I. J. Schoenberg and S. K. Zaremba. On Cauchy's lemma concerning convex polygons. *Canad. J. Math.*, 19:1062–1071, 1967.

[26] D. A. Singer. *Geometry: Plane and Fancy.* Springer-Verlag, New York, 1998.

[27] M. Soss and G. T. Toussaint. Geometric and computational aspects of polymer reconfiguration. *J. Math. Chem.*, 27:303–318, 2000.

[28] E. Steinitz and H. Rademacher. *Vorlesungen über die Theorie der Polyeder.* Springer-Verlag, Berlin, 1934.

[29] G. T. Toussaint. The Erdős-Nagy theorem and its ramifications. In *Proc, 11th Canadian Conference on Computational Geometry*, pages 9–12, Vancouver, Canada, 1999. University of British Columbia. long version available at:http://www.cs.ubc.ca/conferences/CCCG.

[30] E. J. Janse van Rensburg, S. G. Whittington, and N. Madras. The pivot algorithm and polygons: results on the FCC lattice. *J. Physics A: Math. and Gen. Physics*, 23:1589–1612, 1990.

Godfried T. Toussaint
School of Computer Science
McGill University
3480 University St.
Montreal, QC
Canada H3A 2A7
godfried@cs.mcgill.ca

Biographical Sketch: Godfried Toussaint received a Ph.D. from the University of British Columbia in 1972. Since then he has been with the School of Computer Science at McGill University, where his main academic interest is computational geometry. He has been a visiting scholar at Stanford University, University of Montreal, Courant Institute, Simon Fraser University, University of the West Indies, University of Amsterdam, University of Newcastle (Australia), Universidad Politecnica de Madrid, and Universidad Politecnica de Catalunya in Barcelona. He is an editor of several computer science journals and has edited two books and several special issues of journals on computational geometry. In 1978 he received the Pattern Recognition Society's Best Paper of the Year Award, and in 1985, a Killam Fellowship from the Canada Council. In 2001 he received the David Thomson Award for Excellence in Graduate Supervision and Teaching at McGill University. His non-academic interests include, dancing salsa and tango, playing African drums and percussion, scuba diving and travelling.